Journal of Organometallic Chemistry 695 (2010) 1435–1440

Contents lists available at ScienceDirect

Journal of Organometallic Chemistry

journal homepage: www.elsevier.com/locate/jorganchem

Cluster-mediated alkenyl isomerism and carbon–carbon bond formation: The reaction of the unsaturated benzothiazole cluster $[Os_3(CO)_9(\mu_3\text{-}C_7H_4NS)(\mu\text{-}H)]$ with dimethyl acetylenedicarboxylate

Kh. Mahid Uddin [a], Shishir Ghosh [a], Arun K. Raha [a], Graeme Hogarth [b], Edward Rosenberg [c,*], Ayesha Sharmin [c], Kenneth I. Hardcastle [d], Shariff E. Kabir [a,*]

[a] Department of Chemistry, Jahangirnagar University, Savar, Dhaka 1342, Bangladesh
[b] Department of Chemistry, University College London, 20 Gordon Street, London WC1H OAJ, UK
[c] Department of Chemistry, The University of Montana, Missoula, MT 59812, USA
[d] Department of Chemistry, Emory University, Atlanta, Georgia 30322, USA

ARTICLE INFO

Article history:
Received 21 January 2010
Received in revised form 17 February 2010
Accepted 19 February 2010
Available online 24 February 2010

Keywords:
Osmium
Carbonyl
Alkenyl isomerism
Carbon–carbon bond formation
X-ray structures

ABSTRACT

Upon mild heating (60–65 °C), electron-deficient $[Os_3(CO)_9(\mu_3\text{-}C_7H_4NS)(\mu\text{-}H)]$ (**1**) readily adds to the activated alkyne, RC≡CR (R = CO_2Me), to give two isomers of the alkenyl complexes, $[Os_3(CO)_9(\mu\text{-}C_7H_4NS)(\mu_3\text{-}RCCHR)]$ (**2** and **3**), differing in the orientation of the benzothiazole ligand. In both the alkenyl ligand acts as a five-electron donor binding through both carbons and one of the oxygen atoms of the substituents, which adopt a relative *cis* disposition. Heating **2** cleanly affords **3** suggesting that the former is the kinetic product and the latter is thermodynamically favoured. At higher temperatures (110 °C), **3** rearranges to a third isomer $[Os_3(CO)_9(\mu\text{-}C_7H_4NS)(\mu\text{-}RCCHR)]$ (**4**) which differs in the binding mode of the alkenyl ligand and where the alkyne substituents are in a relative *trans* disposition. A second product of this reaction is $[Os_3(CO)_8(\mu\text{-}OCH_3)\{\mu_3\text{-}C_7H_4NSC(R)C\}(\mu\text{-}H)]$ (**5**) which results from the loss of two moles of CO, carbon–carbon coupling between hydrocarbyl and benzothiazole ligands and carbon–hydrogen addition to the triosmium centre. All new clusters are characterized by a total of 50 valence electrons and contain two metal–metal bonds as shown by single crystal X-ray diffraction studies.

1. Introduction

The unsaturated 46-electron cluster $[Os_3(CO)_{10}(\mu\text{-}H)_2]$ [1] has been shown to be highly reactive towards a wide range of substrates. With alkynes, reactions can lead to a number of different products [2–9] with hydrometalation to yield alkenyl complexes being the most prevalent. For example, Dawoodi and Mays [9] have reported that the activated alkyne, $CF_3C{\equiv}CCF_3$, reacts with $[Os_3(CO)_{10}(\mu\text{-}H)_2]$ to afford a zwitterionic alkenyl complex (Eq. (1)), in which the hydrocarbyl fragment caps the osmium triangle. Surprisingly, the reaction of $[Os_3(CO)_{10}(\mu\text{-}H)_2]$ with the activated alkyne, dimethyl acetylenedicarboxylate (dmad) appears not to have been reported.

The benzoheterocyclic clusters $[Os_3(CO)_9(\mu_3\text{-benzoheterocycle})(\mu\text{-}H)]$ represent further examples of unsaturated 46-electron triosmium hydride complexes and over the past 10 years they have been shown to show to be reactive towards a wide range of substrates [10–17]. We have now investigated the reaction of one of these complexes, namely $[Os_3(CO)_9(\mu_3\text{-}C_7H_4NS)(\mu\text{-}H)]$ (**1**) [10], towards the activated alkyne dmad. This results in formation of a series of isomeric alkenyl complexes and finally to the generation of a novel cluster resulting from the coupling of hydrocarbyl and benzothiazole ligands.

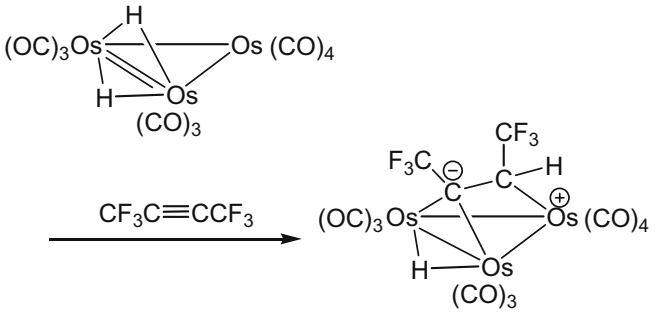

(1)

* Corresponding authors. Tel.: +88 02 7791033; fax: +88 02 7791052.
E-mail address: skabir_ju@yahoo.com (S.E. Kabir).

0022-328X/$ - see front matter © 2010 Elsevier B.V. All rights reserved.
doi:10.1016/j.jorganchem.2010.02.024

2. Experimental

2.1. General data

All reactions were carried out under a dry nitrogen atmosphere using standard Schlenk techniques unless otherwise stated. Reagent grade solvents were dried using appropriate drying agents and distilled prior to use by standard methods. Dimethylacetylenedicarboxylate was purchased from Aldrich and used as received. Cluster $[Os_3(CO)_9(\mu_3\text{-}C_7H_4NS)(\mu\text{-}H)]$ (**1**) was prepared according to the previously reported procedure [10]. Infrared spectra were recorded on a Shimadzu FTIR 8101 spectrophotometer. NMR spectra were recorded on a Varian Unity Plus 400 instrument. Elemental analyses were performed by Schwarzkopf Microanalytical Laboratories, Woodside, NY.

2.2. Reaction of *1* with dimethylacetylenedicarboxylate

To a hexane solution (50 mL) of **1** (150 mg, 0.156 mmol) was added dimethylacetylenedicarboxylate (231 mg, 1.63 mmol) and the mixture was then heated to reflux for 5 h. The solvent was removed under reduced pressure and the residue separated by TLC on silica gel. Elution with hexane/CH_2Cl_2 (1:1, v/v) developed three bands. The first band was unreacted **1** (trace). The second and third bands afforded $[Os_3(CO)_9(\mu\text{-}C_7H_4NS)(\mu_3\text{-}MeO_2CCCHCO_2Me)]$ (**3**) (117 mg, 68%) and $[Os_3(CO)_9(\mu\text{-}C_7H_4NS)(\mu_3\text{-}MeO_2CCCHCO_2Me)]$ (**2**) (36 mg, 21%) in order of elution as yellow crystals after recrystallization from hexane/CH_2Cl_2 at 4 °C. Spectral data for **2**: Anal. Calc. for $C_{22}H_{11}NO_{13}Os_3S$: C, 24.02; H, 1.01; N, 1.27. Found: C, 24.35; H, 1.09; N, 1.34%. IR (ν(CO), CH_2Cl_2): 2088 w, 2068 s, 2029 s, 1995 s, 1983 m, 1961 w cm^{-1}. ^1H NMR (CD_2Cl_2): δ 9.05 (s, 1H), 7.80 (d, J = 7.6 Hz, 1H), 7.38 (d, J = 7.6 Hz, 1H), 6.96 (t, J = 7.6 Hz, 1H), 3.71 (s, 3H), 3.60 (s, 3H), 2.52 (s, 1H). Spectral data for **3**: Anal. Calc. for $C_{22}H_{11}NO_{13}Os_3S$: C, 24.02; H, 1.01; N, 1.27. Found: C, 24.39; H, 1.11; N, 1.38%. IR (ν(CO), CH_2Cl_2): 2086 m, 2065 s, 2032 s, 1990 s cm^{-1}. ^1H NMR (CD_2Cl_2): δ 8.82 (s, 1H), 7.87 (d, J = 7.6 Hz, 1H), 7.48 (d, J = 7.6 Hz, 1H), 7.13 (t, J = 7.6 Hz, 1H), 3.70 (s, 3H), 3.58 (s, 3H), 2.71 (s, 1H).

2.3. Conversion of *2*–*3*

A hexane solution (30 mL) of **2** (15 mg, 0.014 mmol) was heated to reflux for 4 h. A similar chromatographic separation and workup described as above gave **3** (8 mg, 53%) and unreacted **2** (4 mg).

2.4. Thermolysis of *3*

A toluene solution (30 mL) of **3** (50 mg, 0.045 mmol) was heated to reflux for 5 h. The solvent was removed under vacuum and the residue chromatographed by TLC on silica gel. Elution with hexane/CH_2Cl_2 (1:2, v/v) developed four bands. The first and second bands gave $[Os_3(CO)_8(\mu\text{-}OMe)(\mu_3\text{-}C_7H_4NSCCCO_2Me)(\mu\text{-}H)]$ (**5**) (12 mg, 25%) and $[Os_3(CO)_9(\mu\text{-}C_7H_4NS)(\mu\text{-}MeO_2CCHCCO_2Me)]$ (**4**) (24 mg, 48%) in order of elution as yellow crystals after recrystallization from hexane/CH_2Cl_2 at 4 °C. The third band was unreacted **3** (trace) while the content of the fourth band was too small for complete characterization. Spectral data for **4**: Anal. Calc. for $C_{22}H_{11}NO_{13}Os_3S$: C, 24.02; H, 1.01; N, 1.27. Found: C, 24.41; H, 1.09; N, 1.37%. IR (ν(CO), CH_2Cl_2): 2101 w, 2082 s, 2064 w, 2055 w, 2030 m, 2013 s, 1998 m, 1970 w, 1915 w cm^{-1}. ^1H NMR (CD_2Cl_2): δ 8.80 (s, 1H), 8.03 (d, J = 7.6 Hz, 1H), 7.53 (d, J = 7.6 Hz, 1H), 7.21 (t, J = 7.6 Hz, 1H), 4.40 (s, 1H), 3.71 (s, 3H), 3.54 (s, 3H). Spectral data for **5**: Anal. Calc. for $C_{20}H_{11}NO_{11}Os_3S$: C, 23.01; H, 1.06; N, 1.34. Found: C, 23.45; H, 1.15; N, 1.43%. IR (ν(CO), CH_2Cl_2): 2086 s, 2053 s, 2008 s, 1978 m, 1936 m cm^{-1}. ^1H NMR ($CDCl_3$): δ

Table 1
Crystallographic data and structure refinement for **2–5.**

	2	**3**	**4**	**5**
Empirical formula	$C_{22}H_{11}NO_{13}Os_3S$	$C_{22}H_{11}NO_{13}Os_3S$	$C_{22}H_{11}NO_{13}Os_3S$	$C_{20}H_{11}NO_{11}Os_3S$
Formula weight	1099.98	1099.98	1099.98	1043.96
Temperature (K)	173(2)	173(2)	173(2)	173(2)
Wavelength (Å)	0.71073	0.71073	0.71073	0.71073
Crystal system	Monoclinic	Triclinic	Triclinic	Monoclinic
Space group	$P2_1/c$	$P\bar{1}$	$P\bar{1}$	$P2_1/c$
a (Å)	10.6040(10)	9.2091(7)	9.3655(6)	19.073(3)
b (Å)	11.3345(11)	9.8526(7)	9.8301(6)	7.7538(11)
c (Å)	21.993(2)	16.8579(12)	15.8891(9)	17.251(2)
α (°)	90	100.727(1)	92.228(1)	90
β (°)	99.496(2)	96.225(1)	93.757(1)	113.894(3)
γ (°)	90	116.342(1)	118.430(1)	90
Volume (Å^3)	2607.2(4)	1314.72(17)	1279.53(13)	2332.6(5)
Z	4	2	2	4
D_{calc} (Mg m^{-3})	2.802	2.779	2.855	2.973
μ (Mo Kα) (mm^{-1})	14.734	14.609	15.011	16.453
F(0 0 0)	1992	996	996	1880
Crystal size (mm)	0.21 × 0.13 × 0.07	0.39 × 0.16 × 0.13	0.46 × 0.22 × 0.12	0.36 × 0.27 × 0.17
θ Range (°)	1.88–28.31	2.39–28.30	2.47–28.30	2.34–28.42
Limiting indices	$-14 \leqslant h \geqslant 14$, $-15 \leqslant k \geqslant 15$, $-29 \leqslant l \geqslant 29$	$-12 \leqslant h \geqslant 12$, $-13 \leqslant k \geqslant 13$, $-22 \leqslant l \geqslant 22$	$-12 \leqslant h \geqslant 12$, $-13 \leqslant k \geqslant 13$, $-21 \leqslant l \geqslant 21$	$-25 \leqslant h \geqslant 25$, $-10 \leqslant k \geqslant 10$, $-23 \leqslant l \geqslant 23$
Reflections collected	35 523	18 269	17 722	30 916
Independent reflections (R_{int})	6470 (0.0460)	6523 (0.0274)	6324 (0.0456)	5859 (0.0471)
Max. and min. transmission	0.4253 and 0.1479	0.2525 and 0.0697	0.2660 and 0.0550	0.1663 and 0.0665
Data/restraints/parameters	6470/0/363	6523/0/363	6324/0/367	5859/0/327
Goodness of fit on F^2	1.034	1.102	1.053	1.118
Final R indices [$I > 2\sigma(I)$]	R_1 = 0.0236 wR_2 = 0.0562	R_1 = 0.0200 wR_2 = 0.0498	R_1 = 0.0275 wR_2 = 0.0657	R_1 = 0.0291 wR_2 = 0.0680
R indices (all data)	R_1 = 0.0280 wR_2 = 0.0578	R_1 = 0.0219 wR_2 = 0.0505	R_1 = 0.0300 wR_2 = 0.0669	R_1 = 0.0329 wR_2 = 0.0695
Largest difference in peak and hole (e Å^{-3})	1.815 and −0.759	1.003 and −1.269	2.095 and −1.904	2.922 and −1.112

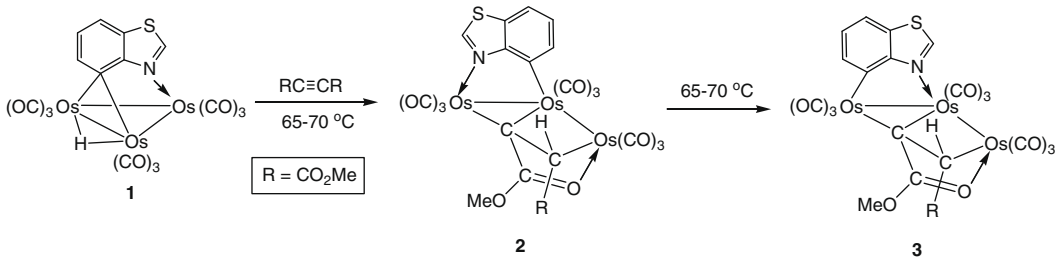

Scheme 1.

9.35 (s, 1H), 8.35 (d, *J* = 7.6 Hz, 1H), 7.88 (d, *J* = 7.6 Hz, 1H), 7.70 (t, *J* = 7.6 Hz, 1H), 3.79 (s, 3H), 2.82 (s, 3H), −14.08 (s, 1H).

2.5. X-ray crystallography

Single crystals of **2**–**5** suitable for X-ray structure were grown by slow diffusion of hexane into dichloromethane solutions at 4 °C. Crystals were coated with Paratone N oil, suspended in a small fiber loop and placed in a cooled nitrogen gas stream at 173 K on a Bruker D8 SMART APEX CCD sealed tube diffractometer with graphite monochromated Mo Kα (0.71073 Å) radiation. Data were measured using a series of combinations of φ and ω scans with 5 s frame exposures and 0.3° frame widths. Data collection, indexing and initial cell refinements were all carried out using SMART [18] software. Frame integration and final cell refinements were done using SAINT [19] software. The final cell parameters were determined from least-squares refinement on 5871 reflections. The SADABS [20] program was used to carry out absorption corrections.

The structure was solved using the Patterson method and difference Fourier techniques (SHELXTL, V6.12) [21]. Hydrogen atoms were placed their expected chemical positions using the HFIX command and were included in the final cycles of least-squares with isotropic Uij's related to the atom's ridden upon. The C–H distances were fixed at 0.93 Å (aromatic and amide), 0.98 Å (methine), 0.97 Å (methylene), or 0.96 Å (methyl). The hydride was positioned by using the XHYDEX program in the WinGX suite of programs [22]. All non-hydrogen atoms were refined anisotropically. Scattering factors and anomalous dispersion corrections are taken from the International Tables for X-ray Crystallography [23]. Structure solution, refinement, graphics and generation of publication materials were performed by using SHELXTL, V6.12 software. Additional details of data collection and structure refinement are given in Table 1.

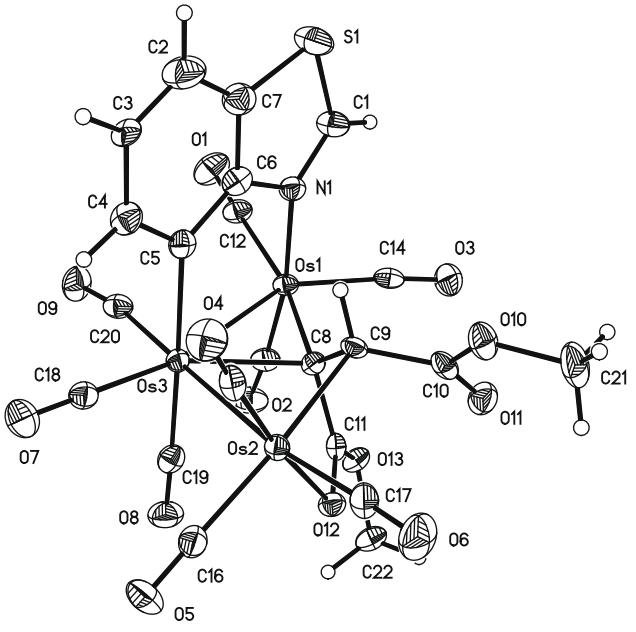

Fig. 1. The solid-state molecular structure of **2** shows 50% probability thermal ellipsoids. Selected interatomic distances (Å) and angles (°): Os(1)–Os(3) 2.8254(3), Os(2)–Os(3) 2.9173(3), Os(2)–O(12) 2.160(3), Os(1)–N(1) 2.127(4), Os(3)–C(5) 2.181(5), Os(2)–C(9) 2.163(4), Os(3)–C(8) 2.251(4), Os(1)–C(8) 2.100(4), C(8)–C(9) 1.520(6), Os(1)–Os(3)–Os(2) 106.575(9), C(11)–O(12)–Os(2) 103.7(3), C(8)–C(9)–Os(2) 90.0(2), Os(1)–C(8)–Os(3) 80.89(14).

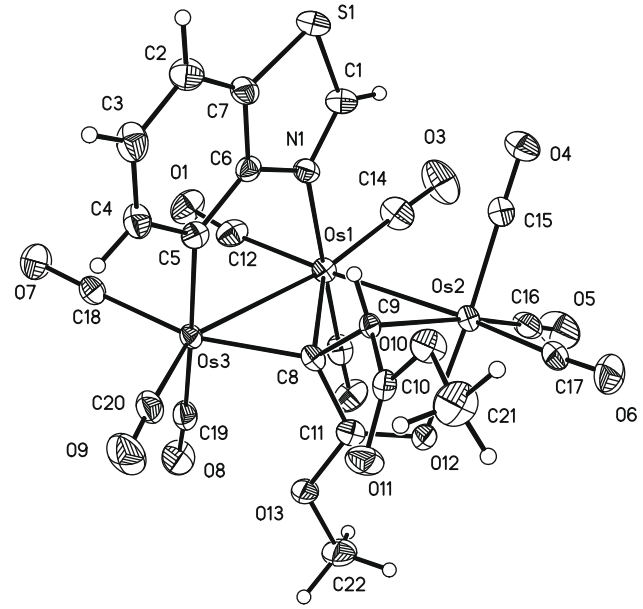

Fig. 2. The solid-state molecular structure of **3** shows 50% probability thermal ellipsoids. Selected interatomic distances (Å) and angles (°): Os(1)–Os(3) 2.8554(2), Os(1)–Os(2) 2.9077(3), Os(2)–O(12) 2.153(2), Os(1)–N(1) 2.178(3), Os(3)–C(5) 2.139(3), Os(2)–C(9) 2.182(3), Os(3)–C(8) 2.102(3), Os(1)–C(8) 2.260(3), C(8)–C(9) 1.534(4), Os(3)–Os(1)–Os(2) 107.688(7), C(11)–O(12)–Os(2) 104.9(2), C(8)–C(9)–Os(2) 91.25(19), Os(1)–C(8)–Os(3) 81.71(11).

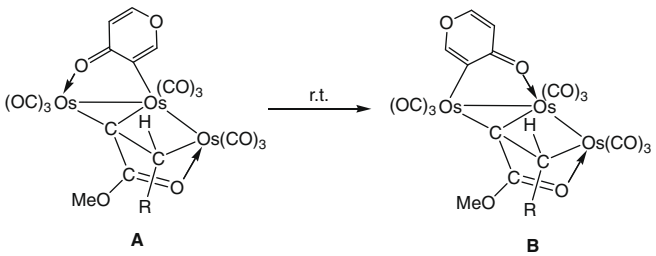

Scheme 2.

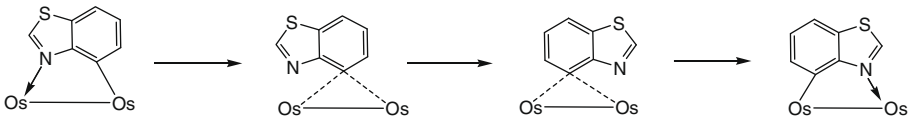

Scheme 3.

3. Results and discussion

3.1. Reaction of $[Os_3(CO)_9(\mu_3\text{-}C_7H_4NS)(\mu\text{-}H)]$ (1) with dmad: isolation of isomers based on the relative orientation of the benzothiazole ligand

Treatment of **1** with excess dmad (RC≡CR, R = CO_2Me) in refluxing hexane led to the isolation of two isomers of the dmad-addition product $[Os_3(CO)_9(\mu\text{-}C_7H_4NS)(\mu_3\text{-}\eta^2,\eta^1,\kappa^1\text{-}MeO_2CCHCO_2Me)]$, *viz.*, **2** (21%) and **3** (68%). In a separate experiment, isomer **2** was shown to cleanly transform to **3** under similar conditions thus establishing **2** as the kinetic product and **3** as the thermodynamic product (Scheme 1). These isomers result from insertion of the alkyne into the metal-hydride with concomitant cleavage of one of the osmium–osmium interactions, metal coordination of an oxygen atom compensating for the formal loss of a metal–metal bond. Hence the overall process converts the 46-electron starting cluster into 50-electron alkenyl clusters.

Both isomers have been crystallographically characterized and their molecular structures are shown in Figs. 1 and 2, respectively, along with selected bond lengths and angles. They consist of an open cluster of three osmium atoms coordinated by nine carbonyls equally distributed to three metal atoms, a $\mu\text{-}C_7H_4NS$ ligand and a $\mu_3\text{-}\eta^2,\eta^1,\kappa^1\text{-}MeO_2CCHCO_2Me$ ligand. The nitrogen atom of the $\mu\text{-}C_7H_4NS$ ligand is bonded to a terminal osmium in **2**, while it is bonded to the central osmium in **3**. In both isomers, the alkenyl ligand is bound to the triosmium core in a $\mu_3\text{-}\eta^2,\eta^1,\kappa^1$ fashion. One carbon, C(8), bridges an osmium–osmium edge which is also bridged by the $\mu\text{-}C_7H_4NS$ ligand. The other alkyne carbon, C(9), is bonded to the third osmium, Os(2) and a hydrogen atom. There is also an additional bonding interaction between a carbonyl oxygen, O(12), of one of the carboxylate group and the third osmium atom, Os(2). In both the doubly bridged osmium–osmium edge is significantly shorter than the other osmium–osmium edge and the carboxylate groups of the hydrocarbyl ligand are located on a different face of the Os_3 triangle with respect to the $\mu\text{-}C_7H_4NS$ ligand. The C(8)–C(9) bond distances [1.520(6) Å in **2** and 1.534(4) Å in **3**] are typical of a carbon–carbon single bond formed by using sp^3 hybrid orbitals. Apparently, the hydride ligand that bridges an osmium–osmium edge in the starting complex **1** has transferred to the alkyne functionality, which can now be considered as a carbon–carbon single bond.

Lin and Leong have very recently reported a similar transformation that occurs upon addition of dmad to the γ-pyrone cluster $[Os_3(CO)_{10}(\mu\text{-}\gamma\text{-}C_5H_3O_2)(\mu\text{-}H)]$ [24]. Here uv photolysis was used to activate the starting cluster towards CO loss and the reaction was very slow. Nevertheless, isomers similar **A** and **B** akin to **2** and **3**, respectively, were produced in which the benzothiazole moiety is replaced by a γ-pyrone ligand. Structural parameters for the two cluster types are essentially identical. Furthermore, a similar conversion of isomers was noted, in this system that occurs at room temperature (no timescale given) (Scheme 2).

The nature of the heterocycle "flipping" in these systems is not clear but a plausible mechanism (Scheme 3) would appear to be the initial release of the heteroatom from the outer osmium atom with the loss of electron-density compensated by the transformation of the metalated carbon atom into a bridging position akin to that found in **1**. Rotation of this group would then place the heteroatom over the central osmium atom. In support of an initial loss of the osmium–heteroatom interaction, the more facile transformation in the γ-pyrone system may be a consequence of the weaker binding of the harder oxygen atom to the triosmium centre as compared to nitrogen. It is also noteworthy that heterocycle "flipping" leads to some subtle changes in the binding of this ligand to the metal centers [Os(3)–C(5) 2.181(5) Å in **2**, Os(3)–C(5) 2.139(3) Å in **3**, Δ = 0.042 Å; Os(1)–N(1) 2.127(4) Å in **2**, Os(1)–N(3) 2.178(3) Å in **3**, Δ = 0.051 Å].

Lin and Leong [24] isolated a third isomer (**C**) from the direct reaction of $[Os_3(CO)_{10}(\mu\text{-}\gamma\text{-}C_5H_3O_2)(\mu\text{-}H)]$ with dmad in which the oxygen of the γ-pyrone ligand is bound to the outer osmium atom and the metal-bound ester group lies on the same side of the triosmium unit as the pyrone ligand (Scheme 4). Interestingly, however, this complex did not undergo isomerisation *via* heterocycle "flipping". This may simply be a consequence of this isomer being more thermodynamically stable than one with the oxygen bound to the central osmium, although in light of the transformations discussed above this does not seem likely. More probably it is

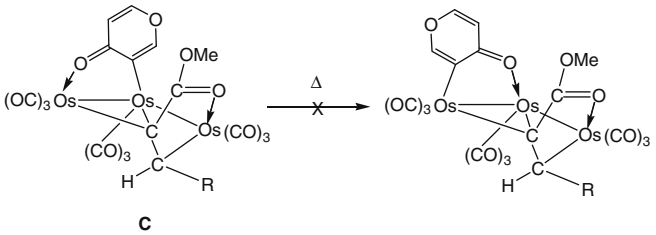

C

Scheme 4.

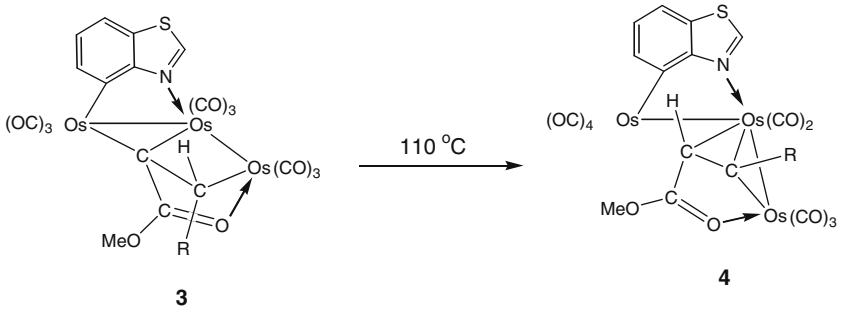

3 4

Scheme 5.

a result of the increased rotational barrier due to the steric encumbrance of the ester ligand.

3.2. Cis–trans alkenyl isomerism

In all the isomeric dmad insertion products discussed above the alkyne substituents adopt a relative *cis* arrangement indicative of a concerted addition of the alkyne to the metal-bound hydride. Heating **3** in toluene results in its conversion to a third isomer **4** in moderate yields (Scheme 5).

The molecular structure of compound **4** is depicted in Fig. 3, and selected bond length and angles are listed in the caption. It is an isomer of compound **3**, and contains a similar triosmium core ligated by nine carbonyls, a bridging μ-C_7H_4NS and μ-MeO_2CCCH-CO_2Me ligands. In **3** the nine carbonyls are equally distributed to three metal centers, but in **4** two are bonded to the central osmium atom while Os(1) and Os(3) have four and three terminal carbonyls, respectively. Also in contrast to **3**, the hydrocarbyl ligand in **4** is coordinated to two metal centers in a μ-η^2,η^1,κ^1 fashion, where the alkyne functionality bridges the Os(2)–Os(3) edge in a σ,π-vinyl fashion [C(14)–C(15) 1.464(6) Å is significantly shorter than the expected sp^3–sp^3 carbon–carbon single bond distance], and has a bond between a carbonyl oxygen, O(7), of one of the carboxylate groups and Os(3). As a consequence, the Os–Os–Os angle is largely expanded in **4** [141.873(8)°] as compared to **2** [106.575(9)°] and **3** [107.688(7)°]. The σ,π-alkenyl coordination mode of the alkyne functionality is also supported by the ^{1}H NMR spectrum which displays a singlet at δ 4.40 (1H) attributable to a vinylic proton bonded to carbon, C(15), whereas the resonance due to this proton appears at δ 2.52 and 2.71 for compounds **2** and **3**, respectively. The μ-C_7H_4NS ligand bridges the Os(1)–Os(2) edge in a similar fashion to that observed in **3**.

Conversion of **3**–**4** involves a 1,2-hydrogen migration within the metal-bound alkenyl ligand [25,26], a process which is associated with carbonyl transfer. We speculate that this process occurs *via* an intermediate metal-hydride complex with the concomitant generation of a bridging alkylidene ligand (Scheme 6). The *cis–trans* isomerisation of metal-bound RC=CHR (R = CO_2Me) has previously been noted at a diiron centre [27].

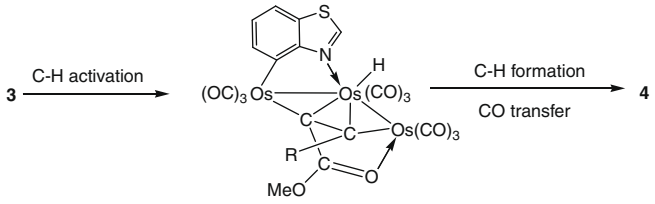

Scheme 6.

3.3. Cluster-mediated coupling of benzothiazole and hydrocarbyl ligands

A second product of the thermolysis of **3** is [$Os_3(CO)_8$(μ-OCH_3)(μ$_3$-$C_7H_4NSCCCO_2Me$)(μ-H)] (**5**) formed by coupling of the benzothiazole and hydrocarbyl ligands and loss of one CO ligand from the metal core as well as one CO from the ester group (Scheme 7).

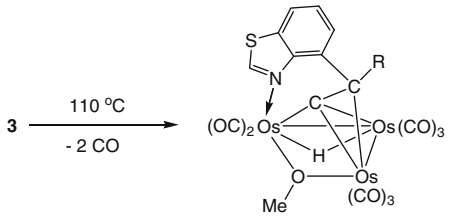

5

Scheme 7.

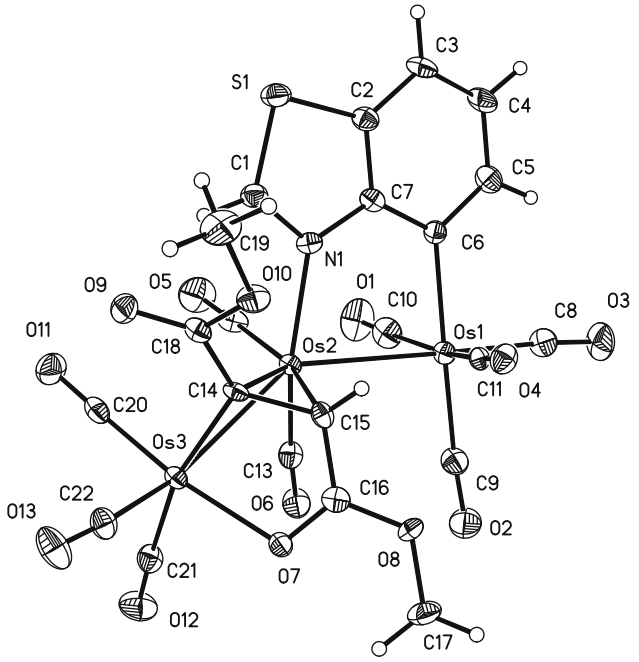

Fig. 3. The solid-state molecular structure of **4** shows 50% probability thermal ellipsoids. Selected interatomic distances (Å) and angles (°): Os(1)–Os(2) 2.8787(3), Os(2)–Os(3) 2.8370(3), Os(3)–O(7) 2.133(3), Os(2)–N(1) 2.170(4), Os(1)–C(6) 2.155(4), Os(2)–C(15) 2.272(5), Os(2)–C(14) 2.166(4), Os(3)–C(14) 2.061(4), C(14)–C(15) 1.464(6), Os(3)–Os(2)–Os(1) 141.873(8), C(16)–O(7)–Os(3) 111.6(3), C(14)–Os(2)–C(15) 38.43(16), Os(3)–C(14)–Os(2) 84.26(15).

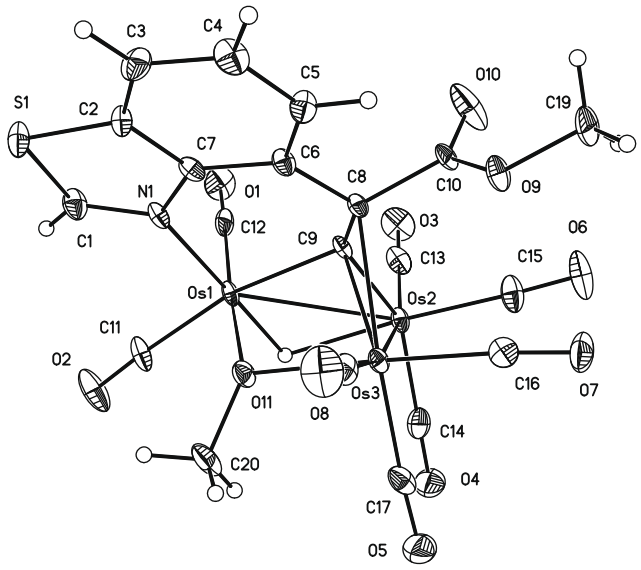

Fig. 4. The solid-state molecular structure of **5** shows the calculated position of the hydride. Thermal ellipsoids were drawn at 50% probability level. Selected interatomic distances (Å) and angles (°): Os(1)–Os(2) 2.8492(4), Os(2)–Os(3) 2.8432(4), Os(1)–O(11) 2.116(4), Os(3)–O(11) 2.114(4), Os(1)–N(1) 2.124(5), Os(1)–C(9) 2.090(5), Os(2)–C(9) 2.013(5), Os(3)–C(9) 2.295(5), Os(3)–C(8) 2.358(5), C(8)–C(9) 1.408(7), Os(3)–Os(2)–Os(1) 72.194(12), C(9)–Os(3)–C(8) 35.20(17), Os(2)–C(9)–Os(1) 88.0(2), Os(2)–C(9)–Os(3) 82.32(19), Os(1)–C(9)–Os(3) 99.7(2), Os(3)–O(11)–Os(1) 104.87(16).

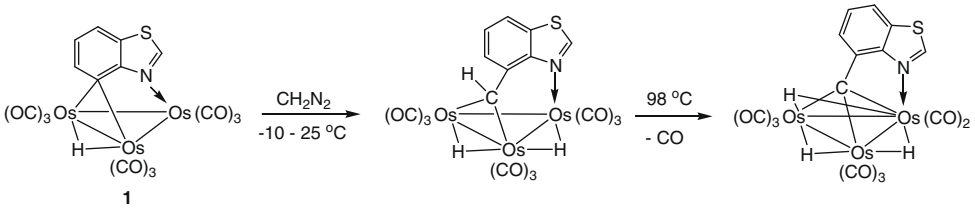

Scheme 8.

The molecular structure of compound **5** is shown in Fig. 4, with selected bond lengths and angles given in the caption. The molecule consists of an open triosmium core coordinated by eight carbonyls, a μ_3-$C_7H_4NSCCCO_2Me$ ligand, and bridging methoxy and hydride ligands. The hydride ligand was located using the program WinGX [22], and is found to span the Os(1)–Os(2) edge. Consistent with this, the ^{1}H NMR spectrum shows a high field singlet at δ −14.08 (1H). The μ-OCH_3 ligand symmetrically bridges the open Os(1)···Os(3) edge [Os(1)–O(11) 2.116(4) Å and Os(3)–O(11) 2.114(4) Å]. An interesting feature of **5** is the presence of a μ_3-$C_7H_4NSCCCO_2Me$ ligand that has been formed by C–C coupling between a carbon of alkyne moiety, C(8), and the C8-carbon [C(6) in the solid-state structure] of the benzothiazole ring. The μ_3-$C_7H_4NSCCCO_2Me$ ligand, which acts as a six electron donor, is coordinated to the trimetallic core through the nitrogen atom of the benzothiazole ring to Os(1), and through the alkyne functionality in such a way that the C(9) carbon of the alkyne functionality bridges the Os(1)–Os(2) edge through two Os–C σ-bonds [Os(1)–C(9) 2.090(5) Å and Os(2)–C(9) 2.013(5) Å] and a η^2 interaction between C(8)–C(9) [1.408(7) Å] and Os(3) [Os(3)–C(9) 2.295(5) Å and Os(3)–C(8) 2.358(5) Å].

Cluster **5** results from a complicated series of transformations including carbon–hydrogen, carbon–carbon and carbon–oxygen bond cleavage and carbon–carbon bond formation. The latter formally results from coupling of an alkynyl and benzothiazole ligand. The alkynyl ligand derives from the cleavage of both hydrogen (trapped as a metal-hydride) and ester (ultimately converted in methoxide and CO) groups from the alkenyl ligand. As far as we are aware, the latter process has not previously been reported. The mode of formation of **5** is complex and thus any comments regarding this can only be speculative. Nevertheless, it is tempting to suggest that formation of **4** and **5** upon thermolysis of **3** may proceed *via* a common intermediate, namely a hydrido–alkylidene complex (Scheme 6). Thus cleavage of the ester group and coupling of the generated alkynyl ligand to the benzothiazole ligand would lead to the formation of **5**.

A related coupling of methylene and benzoheterocylic ligands has previously been seen in related complexes [28–30]. Thus, addition of diazomethane to **1** results in the formation of $[Os_3(CO)_9(\mu_3\text{-}\eta^2\text{-}CHC_7H_4NS)(\mu\text{-}H)_2]$ (Scheme 8) resulting from carbon–hydrogen bond addition to the triosmium cluster and carbon–carbon bond formation [28]. While in this instance no intermediate methylidene complex was observed, in related chemistry such intermediates have been isolated. Further heating of $[Os_3(CO)_9(\mu_3\text{-}\eta^2\text{-}CHC_7H_4NS)(\mu\text{-}H)_2]$ results in a second carbon–hydrogen bond activation to afford $[Os_3(CO)_9(\mu_3\text{-}\eta^2\text{-}CC_7H_4NS)(\mu\text{-}H)_3]$ (Scheme 8). Such carbon–hydrogen bond activation and carbon–carbon bond formation processes are very similar to that noted in the formation of **5** and suggest that this chemistry may be widespread in complexes of this type.

4. Supplementary material

CCDC Nos. 755841 for **2**, 755842 for **3**, 755843 for **4**, 755844 for **5** contain the supplementary crystallographic data for this paper. These data can be obtained free of charge from The Cambridge Crystallographic Data Centre via www.ccdc.cam.ac.uk/data_request/cif.

Acknowledgements

We are grateful to the Ministry of Science and Information & Communication Technology, Government of the People's Republic of Bangladesh for financial support and the Department of Energy (E.R. and A.S. Grant # DE-FG02-01ER45869).

References

[1] H.D. Kaesz, S.A.R. Knox, J.W. Koepke, R.B. Saillant, J. Chem. Soc., Chem. Commun. (1971) 477.
[2] W.G. Jackson, B.F.G. Johnson, J.W. Kelland, J. Lewis, K.T. Schorp, J. Organomet. Chem. 88 (1975) C17.
[3] A.J. Deeming, S. Hasso, M. Underhill, J. Chem. Soc., Dalton Trans. (1975) 1614.
[4] E. Rosenberg, E. Anslyn, L. Milone, S. Aime, R. Gobetto, D. Osella, Gazz. Chim. Ital. 118 (1988) 299.
[5] R.D. Adams, G. Chen, J.T. Tanner, Organometallics 9 (1990) 1530.
[6] E. Sappa, A. Tirripicchio, A.M. Manotti Lanfredi, J. Organomet. Chem. 249 (1983) 391.
[7] J.R. Shapley, Inorg. Chem. 21 (1982) 3295.
[8] R. Gobetto, L. Milone, F. Reineri, L. Salassa, A. Viale, E. Rosenberg, Organometallics 21 (2002) 1919.
[9] Z. Dawoodi, M.J. Mays, J. Chem. Soc., Dalton Trans. (1984) 1931.
[10] M.J. Abedin, B. Bergman, R. Holmquist, R. Smith, E. Rosenberg, K.I. Hardcastle, J. Roe, V. Vazquez, C. Roe, S.E. Kabir, B. Roy, S. Alam, K.A. Azam, R. Duque, Coord. Chem. Rev. 190–192 (1999) 975.
[11] B. Bergman, R. Holmquist, R. Smith, E. Rosenberg, K.I. Hardcastle, M. Visi, J. Ciruash, J. Am. Chem. Soc. 120 (1998) 12818.
[12] E. Rosenberg, E. Arcia, D.S. Kolwaite, K.I. Hardcastle, J. Ciurash, R. Duque, R. Gobetto, L. Milone, D. Osella, M. Botta, W. Dastru, A. Viale, J. Fiedler, Organometallics 17 (1998) 415.
[13] S.E. Kabir, D.S. Kolwaite, E. Rosenberg, K.I. Hardcastle, W. Cresswell, J. Grindstaff, Organometallics 14 (1995) 361.
[14] M.W. Lum, W.K. Leong, J. Chem. Soc., Dalton Trans. (2001) 2476.
[15] M.W. Lum, W.K. Leong, J. Organomet. Chem. 687 (2003) 203.
[16] E. Rosenberg, D. Rokhsana, C. Nervi, R. Gobetto, L. Milone, A. Viale, Chem. Eur. J. 9 (2003) 5749.
[17] E. Rosenberg, D. Rokshsana, C. Nervi, R. Gobetto, L. Milone, A. Viale, J. Fiedler, Organometallics 23 (2004) 215.
[18] SMART Version 5.628, Bruker AXS, Inc., Analytical X-ray Systems, 5465 East Cheryl Parkway, Madison WI 53711-5373, 2003.
[19] SAINT Version 6.36A, Bruker AXS, Inc., Analytical X-ray Systems, 5465 East Cheryl Parkway, Madison WI 53711-5373, 2002.
[20] G.M. Sheldrick, SADABS Version 2.10, University of Göttingen, 2003.
[21] G.M. Sheldrick, Acta Crystallogr. A 64 (2008) 112.
[22] L.J. Farrugia, J. Appl. Crystallogr. 32 (1999) 837.
[23] A.J.C. Wilson, International Tables for X-ray Crystallography, vol. C. Kynoch, Academic Publishers, Dordrecht, 1992 (Tables 6.1.1.4 (pp. 500–502) and 4.2.6.8 (pp. 219–222)).
[24] Q. Lin, W.K. Leong, J. Organomet. Chem. 690 (2005) 322.
[25] S. Doherty, G. Hogarth, J. Chem. Soc., Chem. Commun. (1998) 1815.
[26] M.K. Anwar, G. Hogarth, O.S. Senturk, W. Clegg, S. Doherty, M.R.J. Elsegood, J. Chem. Soc., Dalton Trans. (2001) 341.
[27] G. Hogarth, M.H. Lavender, J. Chem. Soc., Dalton Trans. (1994) 3389.
[28] S.E. Kabir, K.M.A. Malik, H.S. Mandal, M.A. Mottalib, M.J. Abedin, E. Rosenberg, Organometallics 21 (2002) 2593.
[29] M.A. Mottalib, N. Begum, S.M.T. Abedin, T. Akter, S.E. Kabir, M.A. Miah, D. Rokhsana, E. Rosenberg, G.M.G. Hossain, K.I. Hardcastle, Organometallics 24 (2005) 4747.
[30] S.E. Kabir, M.A. Rahman, M.N. Uddin, N. Begum, Ind. J. Chem. 47A (2008) 657.